

Soft Matter

Accepted Manuscript



This is an *Accepted Manuscript*, which has been through the Royal Society of Chemistry peer review process and has been accepted for publication.

Accepted Manuscripts are published online shortly after acceptance, before technical editing, formatting and proof reading. Using this free service, authors can make their results available to the community, in citable form, before we publish the edited article. We will replace this *Accepted Manuscript* with the edited and formatted *Advance Article* as soon as it is available.

You can find more information about *Accepted Manuscripts* in the [Information for Authors](#).

Please note that technical editing may introduce minor changes to the text and/or graphics, which may alter content. The journal's standard [Terms & Conditions](#) and the [Ethical guidelines](#) still apply. In no event shall the Royal Society of Chemistry be held responsible for any errors or omissions in this *Accepted Manuscript* or any consequences arising from the use of any information it contains.

Cholesterol Expels Ibuprofen from the Hydrophobic Membrane Core and Stabilizes Lamellar Phases in Lipid Membranes Containing Ibuprofen

Richard J. Alsop,¹ Clare L. Armstrong,¹ Amna Maqbool,¹
 Laura Topozini,¹ Hannah Dies,¹ and Maikel C. Rheinstädter^{1, *}

¹*Department of Physics and Astronomy, McMaster University, Hamilton, ON, Canada*

(Dated: April 17, 2015)

There is increasing evidence that common drugs, such as aspirin and ibuprofen, interact with lipid membranes. Ibuprofen is one of the most common over the counter drugs in the world, and is used for relief of pain and fever. It interacts with the cyclooxygenase pathway leading to inhibition of prostaglandin synthesis. From X-ray diffraction of highly oriented model membranes containing between 0 and 20 mol% ibuprofen, 20 mol% cholesterol, and dimyristoylphosphatidylcholine (DMPC), we present evidence for a non-specific interaction between ibuprofen and cholesterol in lipid bilayers. At a low ibuprofen concentrations of 2 mol%, three different populations of ibuprofen molecules were found: two in the lipid head group region and one in the hydrophobic membrane core. At higher ibuprofen concentrations of 10 and 20 mol%, the lamellar bilayer structure is disrupted and a lamellar to cubic phase transition was observed. In the presence of 20 mol% cholesterol, ibuprofen (at 5 mol%) was found to be expelled from the membrane core and reside solely in the head group region of the bilayers. 20 mol% Cholesterol was found to stabilize lamellar membrane structure and the formation of a cubic phase at 10 and 20 mol% ibuprofen was suppressed. The results demonstrate that ibuprofen interacts with lipid membranes and that the interaction is strongly dependent on the presence of cholesterol.

Keywords: Ibuprofen, Cholesterol, Lipid Bilayers, Molecular Structure, X-Ray Diffraction

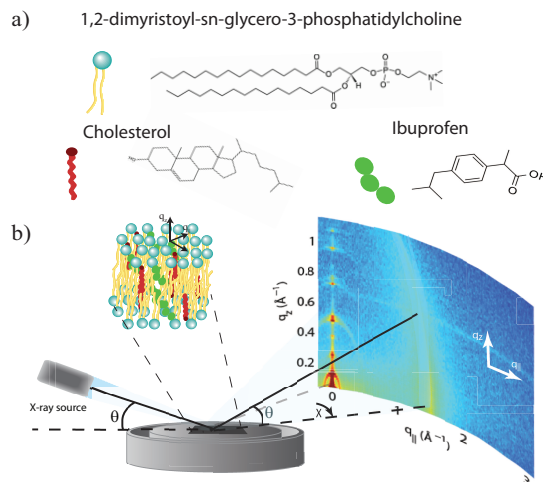


FIG. 1. (a) Schematic representations of dimyristoylphosphatidylcholine (DMPC), cholesterol, and ibuprofen molecules. (b) Diagram of the experimental setup used for X-ray diffraction measurements. Two-dimensional data was obtained to probe the structure of the oriented membrane stack parallel (in-plane) and perpendicular (out-of-plane) to the plane of the membranes.

* Department of Physics and Astronomy, McMaster University, ABB-241, 1280 Main Street West, Hamilton, Ontario L8S 4M1, Canada; Phone: +1-(905)-525-9140-23134, Fax: +1-(905)-546-1252, E-mail: rheinstadter@mcmaster.ca

1. INTRODUCTION

In addition to specific interactions with biochemical targets, many drugs and pharmaceuticals are known to interact with lipid membranes through non-specific molecular interactions^{1,2}. For example, physical interactions with lipid membranes can cause changes to the membrane's fluidity, thickness, or area per lipid^{3,4}. As many biological processes, such as cell signalling and adhesion, are mediated by the membrane and membrane bound proteins, changes to membrane processes induced by drugs can lead to significant changes in their biological function⁵⁻⁹.

When assessing the impact of a foreign molecule (such as a drug) on membrane properties, the partitioning of the drug within the membrane is often crucial. As an example, the common analgesic aspirin has been shown to interact with the head group region of the lipid membrane leading to an increase in lipid fluidity^{10,11}. Aspirin was eventually shown to counteract cholesterol's condensing effect and to redissolve cholesterol plaques in lipid bilayers at high cholesterol concentrations^{12,13}, and also to inhibit formation of cholesterol rafts at physiological concentrations of cholesterol¹⁴. In contrast, the co-surfactant hexanol partitions into the tail group region leading to profound changes in the membrane structure as it induces a lamellar to hexagonal phase transition¹⁵. In particular, small molecules can change partitioning of peptides in membranes. Melatonin was shown to reduce the population of the membrane-embedded state of amyloid- β_{25-35} , a peptide involved in plaque formation in Alzheimer's disease¹⁶.

Ibuprofen is a non-steroidal anti-inflammatory drug

40 (NSAID) who's primary effect is related to the inhibition
 41 prostaglandin synthesis, leading to anti-inflammatory
 42 and pain killing properties^{17,18}. Ibuprofen is a non-
 43 selective inhibitor of the cyclooxygenase enzyme. How-
 44 ever, there is evidence for an interaction of ibuprofen
 45 with lipid membranes. Several studies have reported that
 46 ibuprofen leads to an increase in area per lipid¹⁹ and
 47 membrane defects²⁰, as well as a decreased membrane
 48 bending modulus, κ ²¹.

49 Here, we determine the location of ibuprofen in satu-
 50 rated lipid bilayers at a concentration of 2 mol% and re-
 51 port experimental evidence for an indirect, non-specific
 52 interaction between ibuprofen and cholesterol in mem-
 53 branes containing 5 mol% ibuprofen and 20 mol% chole-
 54 sterol. Through X-ray diffraction in multi-lamellar, ori-
 55 ented membranes, we locate the ibuprofen molecule in
 56 the head group region and the hydrophobic core of the
 57 bilayers and observe that the presence of cholesterol ex-
 58 pels ibuprofen from the membrane core. Cholesterol was
 59 also found to stabilize membrane structure, as the forma-
 60 tion of an inverse cubic phase at high concentrations of
 61 10 and 20 mol% ibuprofen was suppressed when 20 mol%
 62 cholesterol was present.

63 2. RESULTS

64 Highly oriented, multi-lamellar membrane stacks were
 65 prepared on silicon wafers and the molecular structure
 66 was studied using high resolution X-ray diffraction imag-
 67 ing, as depicted in Figure 1. By using oriented mem-
 68 branes, the in-plane (q_{\parallel}) and out-of-plane (q_z) structure
 69 was determined separately, but simultaneously. All mem-
 70 branes were incubated at 30°C in 100% humidity for 24 h
 71 before the measurements and scanned at a temperature
 72 of $T=28^{\circ}\text{C}$ and 50% relative humidity (RH). Similar to
 73 protein crystallography, this dehydrated state suppresses
 74 thermal fluctuations, increases the number of higher order
 75 Bragg peaks and thereby enhances structural fea-
 76 tures, allowing for a high spatial resolution²².

77 Figure 2 shows 2-dimensional reciprocal space maps
 78 for a subset of samples in this study. Measurements are
 79 taken for $-0.3 \text{ \AA}^{-1} < q_{\parallel} < 3 \text{ \AA}^{-1}$ and $0 \text{ \AA}^{-1} < q_z <$
 80 1.1 \AA^{-1} . Pure DMPC membranes are shown in Fig-
 81 ure 2 (a). Some qualitative conclusions can be drawn
 82 from the scattering patterns. The observed scattering
 83 shows a number of well defined intensities along both,
 84 the out-of-plane (q_z) and in-plane (q_{\parallel}) axis, indicative of
 85 lamellar bilayers with strong in-plane ordering.

86 The arrangement of the different molecular compo-
 87 nents in the plane of the membranes can be determined
 88 from the the in-plane scattering along q_{\parallel} . As introduced
 89 by Katsaras and Raghunathan^{23,24}, different molecular
 90 components, such as lipid tails, lipid head groups and
 91 also ibuprofen and cholesterol molecules, can form molec-
 92 ular sub-lattices in the plane of the membrane leading to
 93 non-overlapping sets of Bragg peaks.

94 The 100% DMPC sample in Figure 2 (a) shows a num-

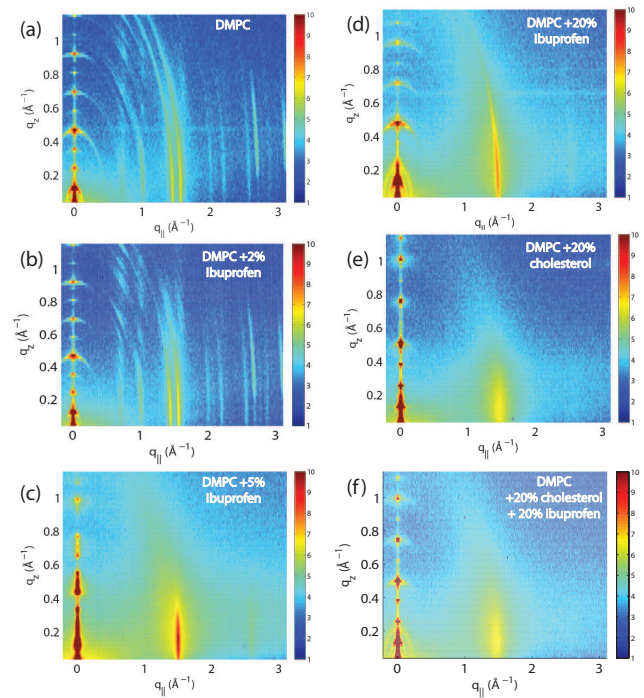


FIG. 2. Reciprocal space maps of selected samples: (a) pure DMPC bilayers; (b) DMPC+2 mol% ibuprofen; (c) DMPC+5 mol% ibuprofen; (d) DMPC+20 mol% ibuprofen; (e) DMPC+20 mol% cholesterol; (f) DMPC+20 mol% cholesterol+20 mol% ibuprofen. While a small concentration of ibuprofen of 2 mol% in part (b) does not alter membrane structure significantly, concentrations of more than 5 mol% induce changes in the in-plane and out-of-plane pattern (parts (c) and (d)). Lamellar membrane structure is stabilized in the presence of cholesterol (parts (e) and (f)).

95 ber of well developed in-plane Bragg peaks along the
 96 q_{\parallel} -axis. The diffracted intensity has a distinct rod-like
 97 shape, typical for a 2-dimensional system. The out-of-
 98 plane scattering along q_z shows pronounced and equally
 99 spaced Bragg intensities due to the multi lamellar struc-
 100 ture of the membranes.

101 As detailed for instance in Barrett *et al.*¹⁰, the in-plane
 102 Bragg peaks can be assigned to two different molecu-
 103 lar lattices, the lipid head groups and the lipid tails:
 104 An orthorhombic head group lattice (planar space group
 105 $p2$) with lattice parameters $a=8.773 \text{ \AA}$ and $b=9.311 \text{ \AA}$
 106 ($\gamma=90^{\circ}$) and a commensurate monoclinic lattice of the
 107 lipid tails with parameters $a_T=4.966 \text{ \AA}$, $b_T=8.247 \text{ \AA}$ and
 108 $\gamma_S=94.18^{\circ}$. The orthorhombic unit cell of the head group
 109 lattice contains two lipid molecules and has an area of
 110 $A_H = a_H b_H = 81.69 \text{ \AA}^2$. The area per lipid can also be
 111 determined from the unit cell of the tails, which contains
 112 one lipid molecule, to $A_T = a_T b_T \sin \gamma_T = 40.84 \text{ \AA}^2$. The
 113 area can be compared to results published by Tristram-
 114 Nagle, Liu, Legleiter and Nagle²⁵, who provided a refer-
 115 ence for the structure of gel phase DMPC membranes.
 116 The authors find an area per lipid of $\sim 47 \text{ \AA}^2$ in fully
 117 hydrated bilayers at $T=10^{\circ}\text{C}$. The membranes in our

118 study were measured at $T=28^\circ\text{C}$, however, de-hydrated
 119 to 50% RH to enhance structural features leading to a
 120 more closely packed gel structure.

121 The sample with 2 mol% ibuprofen in Figure 2 (b)
 122 shows a qualitatively similar pattern indicating that
 123 small amounts of ibuprofen do not lead to a significant
 124 change in membrane structure or topology. However,
 125 membranes prepared with 5 mol% and 20 mol% ibuprofen
 126 in Figures 2 (c) and (d) show a single in plane feature
 127 at $q_{\parallel} = 1.5 \text{ \AA}^{-1}$. This peak is indicative of hexagonal
 128 packing of disordered lipid tails²⁶. Additional reflections
 129 are observed along q_z , indicative of a change in membrane
 130 topology from the lamellar phase. Samples prepared with
 131 20 mol% cholesterol also show disordered in-plane profiles
 132 (Figures 2 (e) and (f)), however, a lamellar q_z pattern.

133 2.1. Electronic Properties of Ibuprofen

134 Ibuprofen is an overall hydrophobic drug consisting of
 135 a large, hydrophobic body consisting of an aromatic ring
 136 and a carbon tail, and a small, hydrophilic head, where
 137 the oxygen groups are located. Ibuprofen was found to
 138 have low partitioning into water and to locate in the
 139 lipid phase²⁷, preferentially in the interfacial region of
 140 the bilayer²⁸.

141 As electromagnetic waves, X-rays mainly interact with
 142 the electronic structure of molecules. Electron distribu-
 143 tions describing the ibuprofen molecule were calculated
 144 using the solved crystal structure of ibuprofen²⁹. The
 145 corresponding structure file is deposited in the Crystal-
 146 lography Open Database with reference number 2006278.
 147 To take into account thermal motion of atoms and elec-
 148 trons, the position of each atom was modeled by a Gaus-
 149 sian distribution with a width (FWHM) of 1 \AA (or, in
 150 the case of samples with cholesterol, 2 \AA) and the corre-
 151 sponding electron distributions were then projected onto
 152 the z -axis. The molecule can be rotated to have any
 153 orientation with respect to the z -axis.

154 When the long axis of the molecule is not tilted with
 155 respect to the z -axis, three Gaussian distributions well
 156 describe the averaged profile, as shown in Figure 3 (a).
 157 The first peak is assigned to the tail region of the ibupro-
 158 fen, the second to the ring structure, and the third peak
 159 to the oxygenated head region. When the ibuprofen
 160 molecule is tilted between 30° and 60° two Gaussians
 161 are required, as depicted in Figure 3 (b)-(c). When the
 162 molecule is tilted 90° , only a single Gaussian is required,
 163 Figure 3 (d). The electronic profiles in Figure 3 describe
 164 the molecule when the thermal motion of each atom is
 165 modelled by a Gaussian with a FWHM of 1 \AA .

166 The Gaussian distributions used to describe the
 167 ibuprofen profiles were then shifted and scaled to fit ob-
 168 served changes in membrane electron density with the
 169 inclusion of ibuprofen. The orientation and position of
 170 all membrane-embedded states can be determined in this
 171 fashion with high accuracy. This technique was used pre-
 172 viously by Dies *et al.*, who used the atomic structures of

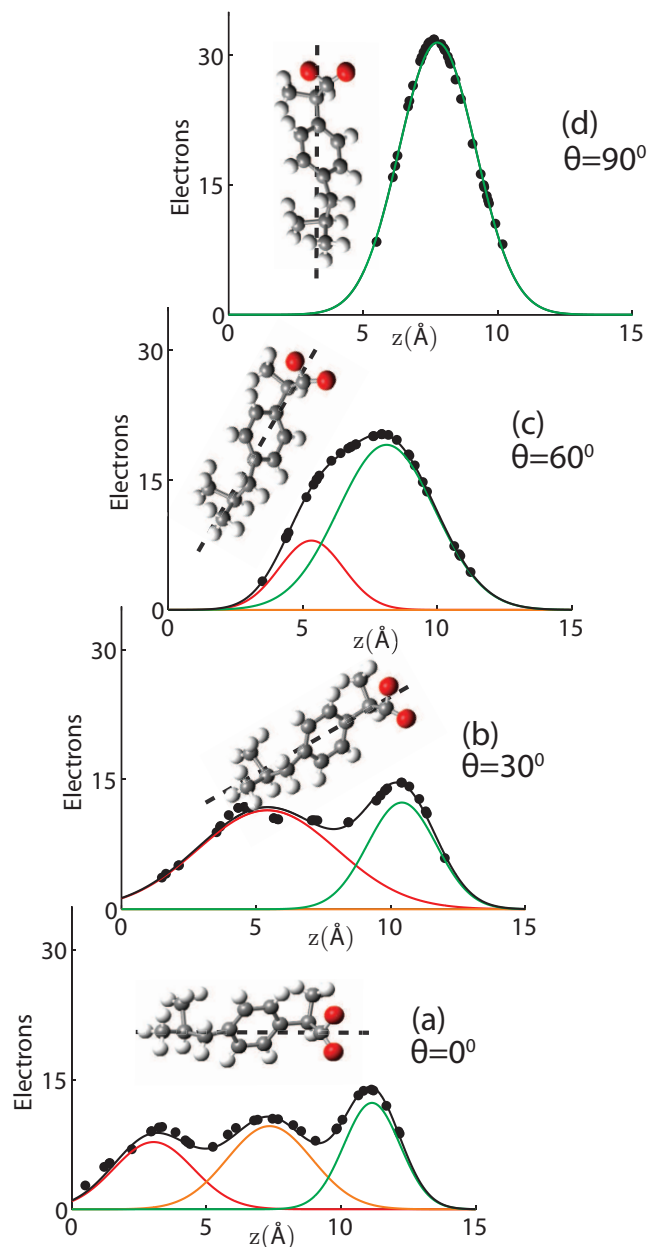


FIG. 3. Gaussian distributions used to describe the electronic distribution of the ibuprofen molecule, projected on the z -axis. Fits are presented when ibuprofen is tilted (a) 0° , (b) 30° , (c) 60° , (d) 90° . Three Gaussians are required to describe the untilted ibuprofen, two Gaussians are needed when the molecule is tilted to 30° or 60° , and one Gaussian is needed when $\theta = 90^\circ$. Dashed lines indicate ibuprofen's long axis. Electronic profiles describe the molecule when the thermal motion of each molecule is modelled by a distribution with FWHM of 1 \AA .

173 amyloid- β peptides and melatonin to determine the lo-
 174 cation of the peptides and enzyme in lipid membranes of
 175 different membrane compositions^{16,30}.

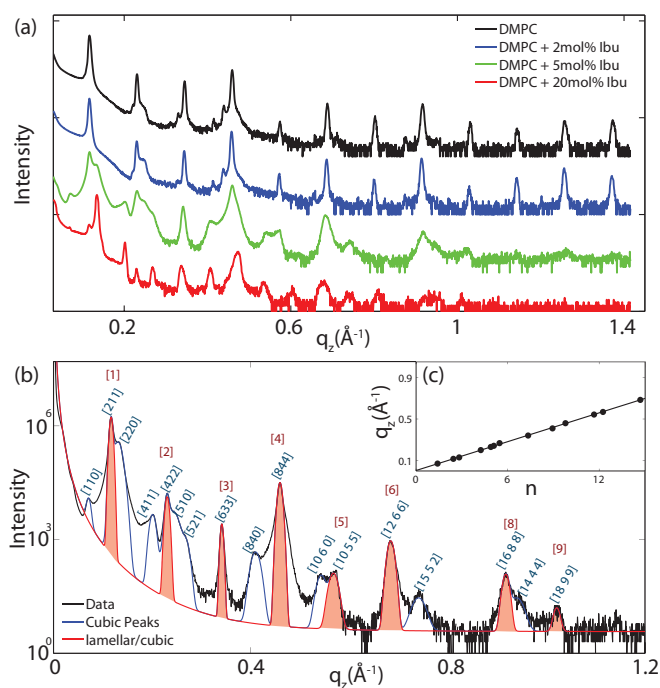


FIG. 4. (a) Out-of-plane X-ray diffraction ($q_{\parallel} = 0 \text{ \AA}^{-1}$) of oriented DMPC membranes containing ibuprofen at concentrations of 0 mol% (black), 2 mol% (blue), 5 mol% (green), and 20 mol% (red). (b) Peak indexing for a membrane with 5 mol% ibuprofen. Gaussian peaks were fit to describe the observed reflectivity curve. Peaks drawn in blue correspond to peaks, which scatter solely from cubic phases. Peaks in red agree with scattering from either a cubic phase or an epitaxially related lamellar phase. The inset (c) shows the position of the peaks along q_z vs. assigned peak indices $(h^2 + k^2 + l^2)^{1/2}$ for a cubic phase. The quality of the peak assignments is shown by the perfectly linear behaviour.

2.2. The Interaction of Ibuprofen with DMPC Membranes

For a quantitative analysis, the 2-dimensional data in Figure 2 were cut along the q_z direction. Out-of-plane diffraction for DMPC membranes prepared with ibuprofen concentrations from 0 mol% to 20 mol% is presented in Figure 4 (a). Up to twelve evenly spaced diffraction peaks were observed for pure DMPC bilayers, indicative of a well ordered lamellar structure. The measured lamellar spacing, d_z , for the pure DMPC was determined to be 55.1 \AA , in agreement with previous reports^{10,25}. A similar pattern is observed for DMPC+2 mol% ibuprofen, which indicates that small amounts of ibuprofen do not change the structure of the bilayers significantly or alter the topology of the membranes. Additional peaks are observed at higher ibuprofen concentrations of 5 mol% and 20 mol% in Figure 4 (a). The structural changes associated with these reflections will be discussed below. The location of the ibuprofen molecules in the saturated lipid bilayers can be determined by comparing the results for pure DMPC and DMPC+2 mol% ibuprofen.

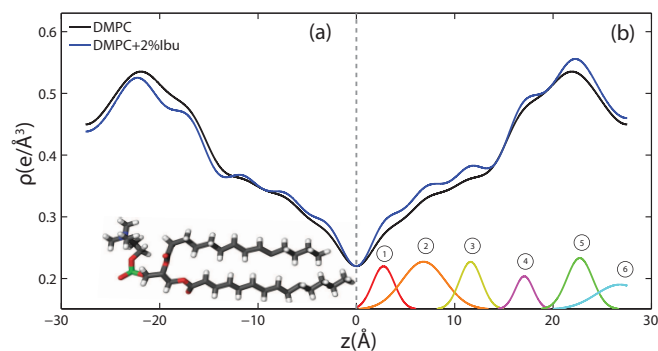


FIG. 5. Electron density profiles for membranes composed of DMPC (black) and DMPC + 2 mol% ibuprofen (blue). Curves on the left, side (a), are on an absolute scale. In (b), the curve representing the membrane prepared with ibuprofen has been scaled by a factor of 1.08 to overlap the profile with that of a pure DMPC membrane (see details in text). The difference between the scaled curve and the DMPC curve is best fit by 6 Gaussian profiles labelled by ① to ⑥.

Electron density profiles of the membranes, $\rho(z)$, were assembled by Fourier synthesis of the observed lamellar Bragg peaks, as detailed in the Materials and Methods Section (Section 4). Bilayer profiles for samples with 0 mol% and 2 mol% ibuprofen are plotted in Figure 5. The profile for a pure DMPC membrane corresponds to a lipid bilayer in the gel state with both chains in an all-trans configuration, as reported previously²⁵. The electron rich phosphorous group in the head region can be identified by the absolute maximum in the electron density profile at $z \sim 22 \text{ \AA}$. ρ_z monotonically decreases to the bilayer centre at $z = 0$, where CH_3 groups reside in the centre with an electron density of $\rho_z = 0.22 e^-/\text{\AA}^3$.

The electron density profiles for both samples are shown in Figure 5 (a) on an absolute scale for $\rho(z)$. There is a general decrease in electron density with the addition of electron-poor ibuprofen and the removal of electron-rich DMPC molecules. The ibuprofen-containing profile was scaled to compensate this overall loss of electron density and to more clearly determine the profile changes induced by the drug, as shown in Figure 5 (b). The electron density profile for 98% DMPC+2 mol% ibuprofen was scaled such that it modelled a pure DMPC (100% DMPC+2 mol% ibuprofen). The difference curve between the scaled profile with ibuprofen and the unscaled DMPC profile shows an increase in electron density due to ibuprofen in both the head group and tail regions which is well modelled by 6 Gaussian distributions, marked by ① to ⑥. Regions of the bilayer profile without ibuprofen molecules coincide with the pure DMPC bilayer in part (a).

The electronic distribution of an ibuprofen molecule can be fit to the difference curve to determine the position and orientation ibuprofen molecules. Three embedded states were observed. Three of the observed Gaussian distributions at $z = 3 \text{ \AA}$, 7 \AA , and 11.5 \AA were assigned to a single ibuprofen molecule residing in the hydrophobic

233 membrane core, oriented parallel with the bilayer z -axis,
 234 with a tilt angle of $0 \pm 5^\circ$. In addition to changes in the
 235 tail regions, two additional increases in electron density
 236 were observed in the head group region. A single peak is
 237 observed at $z=17 \text{ \AA}$, best described by a bound ibuprofen
 238 molecule, rotated by $90^\circ \pm 11^\circ$ with respect to the z -axis,
 239 at the interface of the head group and tail group regions.
 240 Two peaks at $z=23 \text{ \AA}$ and $z=27 \text{ \AA}$ are best described by
 241 a molecule which is distributed between the two bilayers
 242 and aligned with the z -axis (tilt of $0 \pm 5^\circ$). The peak at
 243 $z=23 \text{ \AA}$ is described by the electron distribution of both
 244 the hydroxyl group and the terminal methyl groups of
 245 an ibuprofen molecule, suggesting both portions of the
 246 molecule are observed embedded in the head groups (of
 247 opposite bilayers). The peak at $z=27 \text{ \AA}$ suggests the ring-
 248 group of ibuprofen observed between bilayers. A cartoon
 249 depicting the three membrane bound states for ibuprofen
 250 is shown in Figure 9 (a). By integrating the area under
 251 the peaks observed in the difference electron density
 252 curve, the relative occupation of each bound state can be
 253 determined. A relative occupation of 56% is observed for
 254 the upright state in the tails, 8% for the rotated state at
 255 the head-tail interface, and 36% for the state in the head
 256 groups.

257 .
 258 Figure 4 (b) shows the out-of-plane diffraction pattern
 259 obtained from a membrane prepared with 5 mol% ibuprofen
 260 in a pure DMPC membrane. All observed peaks are
 261 fit with Gaussian peak profiles. The observed peaks can-
 262 not be indexed by a pure lamellar phase, however, may be
 263 indexed to a $Im\bar{3}m$ cubic structure with lattice param-
 264 eter $a = 134 \text{ \AA}$. The corresponding cubic phase Miller
 265 indices are given on the Figure; however, select peaks are
 266 indexed by a lamellar phase with bilayer spacing of $d_z =$
 267 55.1 \AA . These peaks are indicated by red Gaussian profiles
 268 in Figure 4 (b). Peaks solely indexed by the cubic
 269 phase are described by blue profiles. Note that the spac-
 270 ing of the [211] plane of cubic phases is often observed to
 271 be epitaxially related to the bilayer spacing of the lamel-
 272 lar phase. The position, d -spacing, and Miller indices for
 273 all peaks extracted from Figure 4 (b) are listed in Table 1.

274 To determine the relation between cubic and lamellar
 275 phase and the orientation of both phases, 2-dimensional
 276 X-ray maps of the region of interest were obtained for
 277 membranes with 0 mol%, 10 mol%, and 20 mol% ibuprofen,
 278 and are displayed in Figure 6. The plots show the
 279 region $0 < q_z < 0.21 \text{ \AA}^{-1}$ and $0 < q_{||} < 0.21 \text{ \AA}^{-1}$ in more
 280 detail, as compared to the overview plots in Figure 2.
 281 The pure DMPC bilayers in Figure 6 (a) show the lamel-
 282 lar $[100]_L$ Bragg peak and two diffuse contributions: The
 283 lamellar diffuse scattering occurring in horizontal sheets
 284 is the result of bilayer undulation dynamics. Bilayers,
 285 which are not perfectly oriented parallel to the silicon
 286 substrate lead to a faint powder ring, labeled as “defect
 287 scattering”. The number of these defect bilayers is typi-
 288 cally very small as evidenced by the logarithmic intensity
 289 plot.

290 In addition to the cubic peaks observed in the out-of-

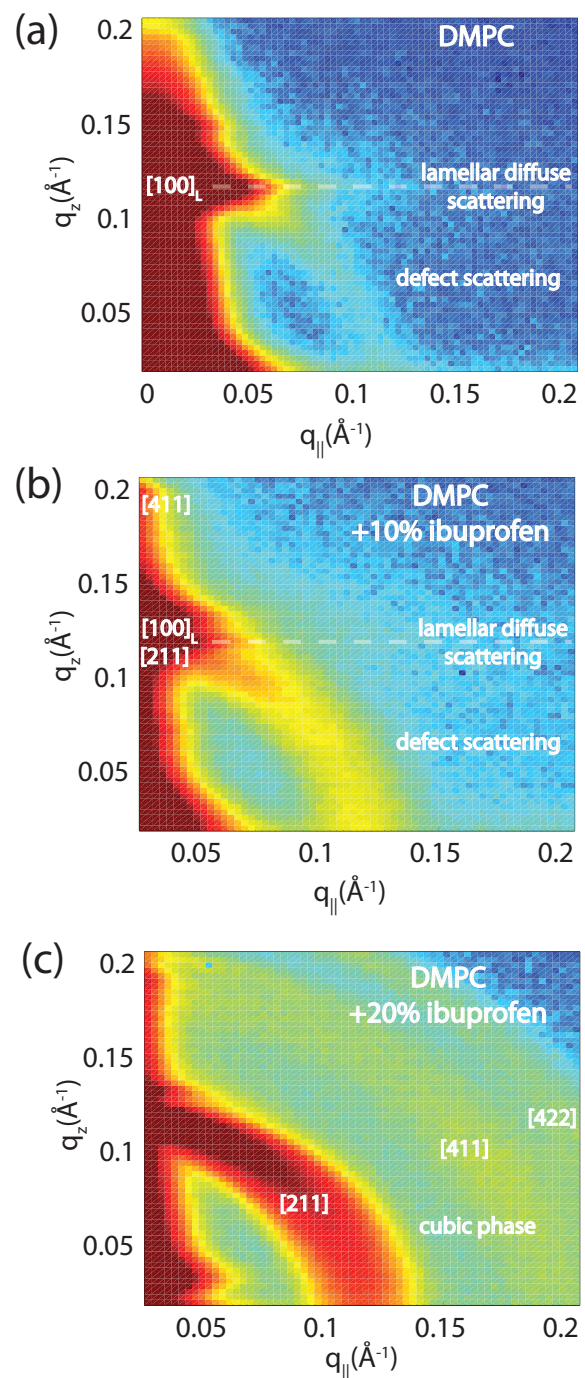


FIG. 6. High resolution reciprocal space maps show the increase in powder scattering with increased ibuprofen. Bilayers were prepared with concentrations of: (a) 0 mol%; (b) 10 mol% and (c) 20 mol% ibuprofen. Only a lamellar peak is observed for pure DMPC. The observed diffuse scattering was attributed to lamellar diffuse scattering due to fluctuations and defect scattering as the result of a small fraction of bilayers not perfectly aligned on the substrate³¹. For a membrane with 10 mol% ibuprofen, the defect scattering significantly increased indicative of a large fraction of “misaligned” bilayers. A cubic pattern is observed at 20 mol% ibuprofen. Intensities are shown on a logarithmic scale.

q_z -position (\AA^{-1}) (\AA^{-1})	d -spacing (\AA) (\AA)	Miller Index
0.077	88.3	[110]
0.117	53.7	[211]
0.131	48.1	[220]
0.201	31.2	[411]
0.231	27.2	[422]
0.242	25.9	[015]
0.268	23.4	[521]
0.342	18.4	[633]
0.410	15.3	[840]
0.460	13.7	[844]
0.543	11.6	[10 6 0]
0.568	11.1	[10 5 5]
0.684	9.18	[12 6 6]
0.741	8.48	[2 5 15]
0.918	6.84	[16 8 8]
0.940	6.68	[4 14 14]
1.021	6.15	[18 9 9]

TABLE 1. Peak position, d -spacing, and assigned Miller index for the reflectivity peaks measured from 5 mol% ibuprofen. All peaks are well described by a cubic phase with space group $Im\bar{3}m$ and $a=134 \text{ \AA}$.

plane curves in Figure 4, there is a drastic increase in the intensity of defect scattering with increasing ibuprofen content (DMPC+10 mol% ibuprofen is shown in Figure 6 (b)), indicating an increase of membranes, which have a random orientation with respect to the perpendicular z -axis. While cubic peaks were observed in the specular out-of-plane scans, no diffuse cubic signals are visible in the 2-dimensional data at this ibuprofen concentration, most likely because the volume fraction of the cubic phase is still small. The pattern at 10 mol% ibuprofen is indicative of a coexistence of lamellar and cubic phases.

A distinct cubic peak pattern is observed at 20 mol% ibuprofen in Figure 6 (c). The positions of the broad powder-rings agree with cubic peaks observed in reflectivity measurements: the [211], [411], and [422] peaks are observed corresponding to a cubic phase (see Figure 4 (b)). The faint [110] and [220] peaks observed in out-of-plane curves could not be resolved from the more diffuse in-plane scattering.

2.3. The Interaction of Ibuprofen with Membranes Containing Cholesterol

Because ibuprofen molecules were found to partition in pure lipid bilayers, DMPC membranes with cholesterol concentrations of 20 mol% and between 0 mol% to 20 mol% ibuprofen were prepared to study a potential interaction between cholesterol and ibuprofen. Out-of-plane diffraction scans for DMPC+20 mol% cholesterol, DMPC+20 mol% cholesterol+5 mol% ibuprofen and DMPC+20 mol% cholesterol+20 mol% ibuprofen are

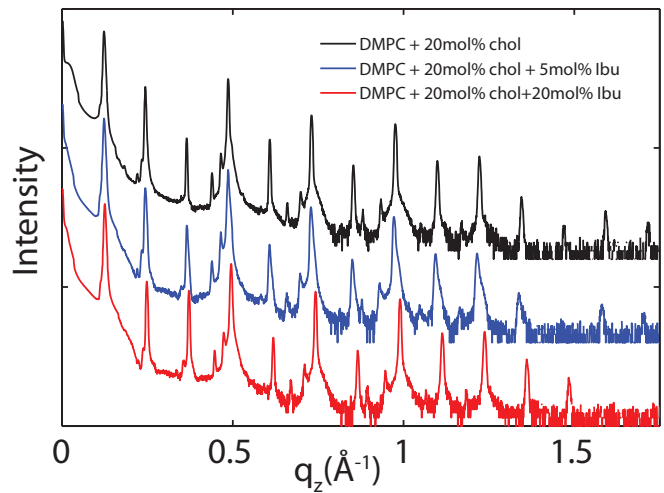


FIG. 7. Out-of-plane diffraction for bilayers prepared with 20 mol% cholesterol and ibuprofen concentrations of: (a) 0 mol%, (b) 5 mol%, (c) 20 mol%.

plotted in Figure 7. The diffraction patterns could all be indexed by lamellar phases. Electron density profiles for 0 mol% and 5 mol% ibuprofen were used to determine the position of the ibuprofen molecule in cholesterol-containing DMPC membranes and are shown in Figure 8 (a). The curve containing ibuprofen in Figure 8 (b) was scaled to represent a DMPC+20 mol% cholesterol bilayer with 5 mol% ibuprofen embedded, as in Section 2.2. The difference between this scaled curve and the curve without ibuprofen was used to locate ibuprofen in membranes with cholesterol. Note that for membranes with cholesterol, when modelling the electronic distribution of ibuprofen for fitting to the difference curve each atom is modelled by a Gaussian distribution with a width of 2 \AA , as opposed to 1 \AA for membranes without cholesterol. The need for increased Gaussian blurring is most likely a consequence of increased molecular disorder with the addition of cholesterol to gel phase membranes¹³.

Two Gaussian distributions, centred at $z=15 \text{ \AA}$ and at 26 \AA , were found to well describe the difference in electron density and were modelled as membrane embedded states for ibuprofen. The location of these states is in excellent agreement with the head group states observed in bilayers without ibuprofen in Section 2.2. The peak at $z=15 \text{ \AA}$ is best described by an ibuprofen molecule tilted by $90^\circ \pm 1$ relative to the bilayer normal, as depicted in the electron distribution calculations in Figure 3 (b). The peak at $z=26 \text{ \AA}$ describes an ibuprofen molecule oriented parallel with the z -axis, and embedded between bilayers (tilt of $0^\circ \pm 1$), similar to the bilayer spanning state observed in membranes without cholesterol. Note that the two membrane electron density profiles in Figure 8 (b) coincide in the tail group region, suggesting that ibuprofen does not occupy this region in the presence of cholesterol. By comparing the integrated intensity of the corresponding Gaussian peaks, the relative occupations of the states

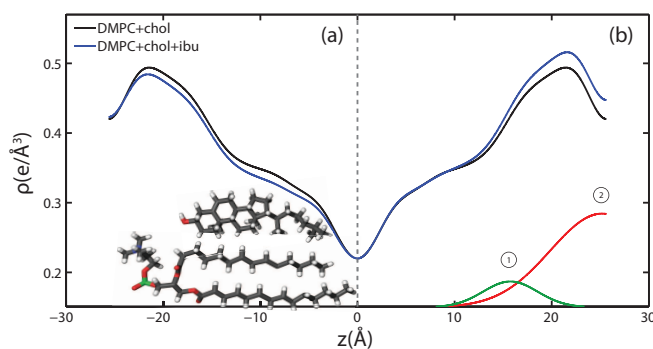


FIG. 8. Electron density profiles for DMPC membranes prepared with 20 mol% cholesterol (black) and 20 mol% cholesterol with 5 mol% ibuprofen (blue). The curves in (a) are on an absolute scale, while the ibuprofen containing curve in (b) was scaled to overlap the profile with that of a 20 mol% cholesterol-containing DMPC membrane (see details in text). The difference between the scaled curve and the black curve is best described by two Gaussian profiles, which are labelled in (b).

at $z=15$ Å and $z=26$ Å are 14% and 86%, respectively.

3. DISCUSSION AND CONCLUSIONS

Structural parameters, such as the lamellar spacing, d_z , the cubic spacing and the area per lipid, A_L were determined for all samples and are listed in Table 2. Ibuprofen was found to not change d_z and A_L in gel DMPC bilayers for the concentrations used and within the resolution of this experiment. Addition of 20 mol% cholesterol led to an increase in lipid area and a decrease of lamellar spacing, as reported previously for gel phase bilayers¹³. The presence of 20 mol% cholesterol was found to suppress the formation of a cubic phases when up to 20 mol% ibuprofen was incorporated as well.

3.1. Partitioning of Ibuprofen in Saturated Lipid Membranes With and Without Cholesterol

The partitioning of ibuprofen in gel phase DMPC membranes was determined using a combination of X-ray diffraction and electronic structure calculations using crystallographic ibuprofen data. The result is summarized in Figure 9. While the peak amplitudes in the calculated profiles in part (a) appear to be systematically slightly smaller than the measured differences, peak position and peak widths show an excellent agreement. Based on the electronic properties in Section 2.1, the orientation of the ibuprofen molecules can be determined: while 3 peaks in the electron density difference indicate a parallel orientation, a single peak is consistent with a perpendicular, 90° orientation.

Three different membrane bound populations were observed when 2 mol% ibuprofen were added to the DMPC

bilayers, as sketched in Figure 9 (a): ① a state in the hydrophobic membrane core, where the ibuprofen molecules align parallel to the lipid acyl chains; 56% of ibuprofen molecules were found in this state; ② 8% of ibuprofen molecules were observed at the interface between head groups-tail groups, and ③ 36% of ibuprofen molecules were found attached to the membrane head group region, situated between the lipid head groups of two bilayers. At ibuprofen concentrations greater than 5 mol% (10 and 20 mol%), disruption of the lamellar membrane phase and the formation of a cubic lyotropic phase was observed.

Based on a fit of the molecular electronic distribution of the ibuprofen molecule to the experimental data, as depicted in Figure 3, the ibuprofen molecules in the hydrophobic membrane core align parallel to the lipid tails, with their hydrophilic head groups located in the head group region of the bilayers (population ①). The 180° position, where the oxygen groups would locate in the bilayer centre, was found to be less favourable with a χ^2 value of $6.33 \cdot 10^4$, as compared to $\chi^2 = 4.28 \cdot 10^4$ for the 0° case. The locations of the ibuprofen molecules are consistent with previous studies, where ibuprofen was reported to associate with PC lipids^{3,27}. Based on electrostatic considerations, the hydrophilic head of the ibuprofen is likely to locate in the head group region of the bilayers^{19,28}. Population ③ corresponds to a state, where the ibuprofen molecule appears to be partially embedded in the head groups of two lipid bilayers, with the hydroxyl group in one bilayer and the terminal methyl groups in another. This membrane-spanning state of ibuprofen is likely a consequence of the stacked bilayers used for the diffraction experiments.

Only two populations of ibuprofen molecules were observed in the presence of cholesterol, as depicted in Figure 9 (b). 14% of the ibuprofen molecules were found to occupy a state at the head group-tail group interface (population ②), while 86% of the molecules were found in the space between two bilayers, attached to the head group region (population ③). While the two states are in agreement with states ② and ③ observed with no cholesterol, no membrane embedded ibuprofen state was observed in the cholesterol-containing lipid bilayers. The presence of cholesterol in the membrane seems to suppress partitioning of ibuprofen into the tail region. As ibuprofen and cholesterol molecules compete for the same space, cholesterol seems to have a higher affinity for the lipid acyl chains.

X-ray diffraction has been used previously to determine the position of a similar NSAID, aspirin, in DMPC membranes with and without cholesterol^{10,12}. Aspirin was found to reside exclusively in the lipid head group region. However, there is a large hydrophobic component to the ibuprofen molecule, which would increase its affinity for the hydrophobic membrane core. Previous simulations of membrane systems incorporating ibuprofen locate the molecule in the tail group regions^{21,32}. In addition, Langmuir isotherm experiments have also sug-

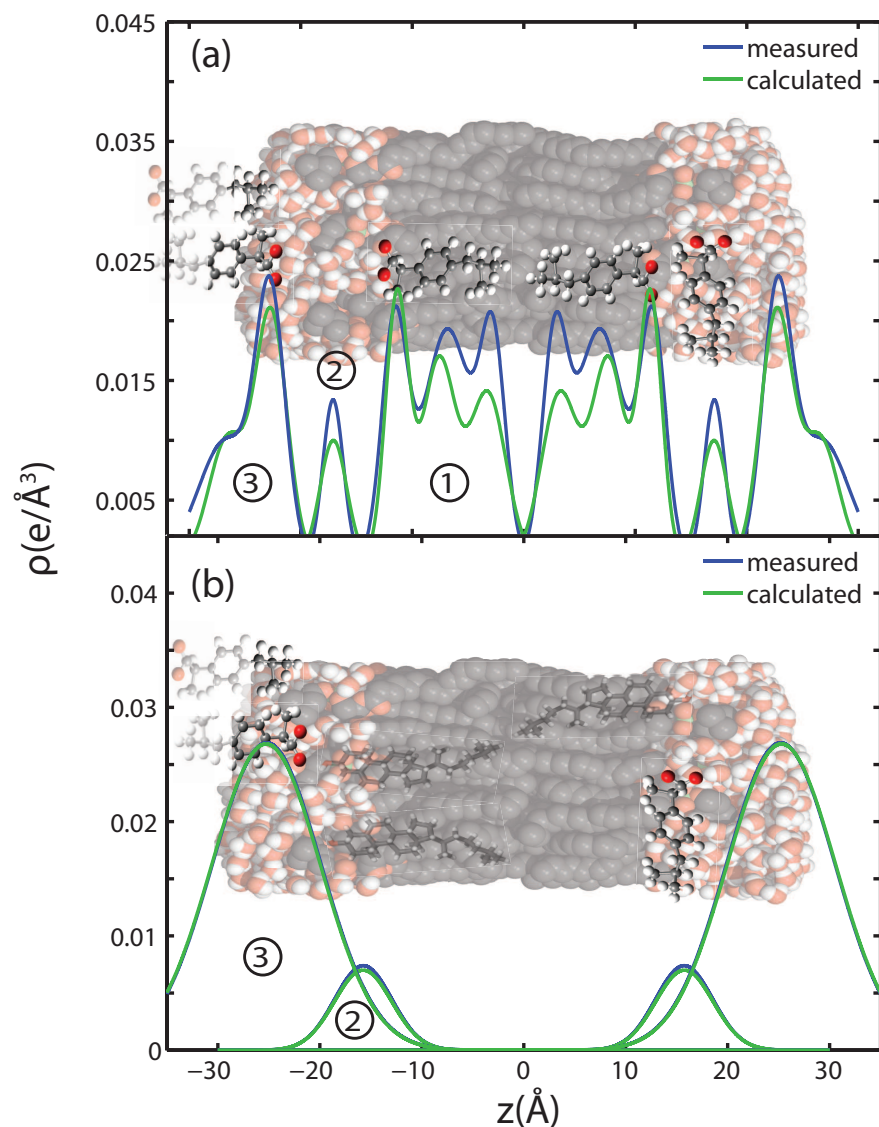


FIG. 9. Measured difference in electron density with the addition of ibuprofen to DMPC membranes and calculated electron distributions of ibuprofen molecules. (a) Three membrane bound states are fit to changes in electron density when 2 mol% ibuprofen is added to pure DMPC bilayers. The calculations take into account ibuprofen molecules, which extend into and are shared with neighbouring bilayers. (b) Two embedded states are fit to the observed changes in electron density when 5 mol% ibuprofen is added to a membrane composed of DMPC+20 mol% cholesterol.

gested that ibuprofen may partition into the head group regions of lipid monolayers³³.

Our results agree qualitatively with other reports. Simulations by Khajeh *et al.* report that the relative position of ibuprofen shifts towards the head groups in DMPC membranes containing 25 mol% cholesterol³². Additional studies have suggested that drug-membrane interactions are significantly influenced by the presence of cholesterol^{34,35}. Our experiments present experimental evidence that cholesterol influences the position of ibuprofen in the membrane and, as will be described below, also suppresses the cubic phase induced by ibuprofen.

3.2. The Suppression of Cubic Phases by Cholesterol

Inverse (type II) phases, such as inverse cubic or inverse-hexagonal phases, are frequently observed in amphiphile-water systems, including systems with lipids, surfactants, and block co-polymers³⁶⁻³⁸. A lamellar to cubic phase transition may be induced in membranes by temperature or pressure jumps in systems containing lipids with negative curvature^{39,40}. Alternatively, inverse phases can be induced by the addition of a largely hydrophobic co-surfactant^{15,41,42}. The fingerprint of a lamellar to cubic phase transition is the appearance of Bragg peaks in diffraction experiments which require 3-fold symmetry to properly index⁴³.

Oriented membranes with ibuprofen concentrations less than 5 mol% formed lamellar phases, while samples with concentrations greater than 5 mol% could not be indexed by a single 1-dimensional lamellar phase and re-

quired a 3-dimensional cubic phase to index all peaks. The observed Bragg peaks for all samples in the cubic phase are consistent with either $Im\bar{3}m$ or $Pn\bar{3}m$ space groups, which are frequently observed in membrane systems^{36,43,44}. The [111] peak, which we did not observe, is systematically absent for $Im\bar{3}m$ but not $Pn\bar{3}m$, suggesting $Im\bar{3}m$ is the best candidate. Another frequently observed cubic phase, with space group $Ia\bar{3}d$, did not describe the peaks as the [110] reflection (absent for $Ia\bar{3}d$) was observed^{44,45}.

In membranes prepared on a solid substrate, where the lamellar phase is oriented, Bragg scattering from the membrane stack is observed solely along the out-of-plane axis, q_z . However, the formation of 3-dimensional cubic phases leads to the appearance of off-specular scattering. Typically, cubic phases form as grains with random orientation, resulting in powder scattering, although oriented cubic phases have been prepared⁴⁶. Two-dimensional measurements of reciprocal space were collected to observe off-specular scattering in the presence of ibuprofen and are depicted in Figure 6. The maps highlight the monotonic increase in powder scattering with increasing ibuprofen concentration. This suggests that increasing ibuprofen leads to cubic phases with grains at random orientation.

While specular peaks can unambiguously be indexed by cubic phases for ibuprofen concentrations greater than 5 mol%, we note that a subset of those peaks may be indexed by a lamellar phase with bilayer spacing in close agreement with samples displaying a pure lamellar phase. The [211] plane of cubic phases is often observed to be epitaxially related to a bilayer spacing in systems with a lamellar to cubic transition^{39,44,47}. Figure 4 (b) demonstrates how the observed peaks are indexed by either a cubic phase, or a cubic phase and a lamellar phase. The experiments, therefore, do not rule out the possibility of a lamellar phase coexisting with the cubic phase. From the 2-dimensional diffraction data in Figure 6 it seems that the formation of cubic phases is accompanied by the a distortion of the lipid bilayers phase and the occurrence of bilayers not parallel to the z -axis.

There is evidence that the impact of certain drugs on the lipid membrane is dependent on membrane composition. For example, negatively charged lipids have been shown to accelerate the binding of the antimicrobial peptide Lacticin Q⁴⁸. In addition, the anti-cancer drug Taxol has a different impact on saturated model membranes and unsaturated membranes⁴⁹. In a recent paper by Khajeh *et al.*, molecular dynamics (MD) simulations were performed on membranes with cholesterol and ibuprofen³² and report that the permeation of ibuprofen across the membrane is decreased by an increased stiffness of the membrane caused by cholesterol.

An increase in chain rigidity and decrease in permeability with the inclusion of cholesterol could explain the reduced penetration depth of Ibuprofen into the membrane^{32,50}. In addition, a change in the position of ibuprofen could explain why cholesterol suppresses cubic

DMPC (mol %)	Ibuprofen (mol %)	Cholesterol (mol %)	d_z (Å)	cubic spacing (Å)	A_L (Å ²)
1	0	0	55.1		40.84
2	2	0	55.1		40.84
3	5	0	55.3	135.7	40.5
4	10	0	56	137	40.5
5	20	0	–	135.7	40.5
6	0	20	51.3		42.5
7	5	20	51.7		42.5
8	20	20	50.9		42.5

TABLE 2. Lamellar spacings and area per lipid are provided for all samples examined. For samples with cubic symmetry, the bilayer repeat distance was calculated using peaks which fit a lamellar spacing.

phase formation. Cholesterol itself has not been shown to suppress cubic phases in membranes with inherently negative curvature⁵¹. However, by causing ibuprofen to partition in the head groups as opposed to the tail groups, cholesterol may prevent the negative curvature or decrease in bending modulus induced by ibuprofen. Our results demonstrate how a membrane constituent, such as cholesterol, can influence the membrane impact of a drug, such as ibuprofen, by changing the partitioning of the drug. Cholesterol can, therefore, act as a protective agent, by inhibiting cubic phases even when ibuprofen is present in high concentration.

4. MATERIALS AND METHODS

4.1. Preparation of the Multi-Lamellar Membranes

Highly oriented, multi-lamellar membranes were prepared on polished 2×2 cm² silicon wafers. The wafers were first pre-treated by sonication in dichloromethane (DCM) at 310 K for 25 minutes to remove all organic contamination and create a hydrophobic substrate. After removal from the DCM post-sonication, each wafer was thoroughly rinsed three times by alternating with ~50 mL of ultra pure water and methanol.

1,2-dimyristoyl-sn-glycero-3-phosphocholine (DMPC) and cholesterol were obtained from Avanti Polar Lipids and individually dissolved in 1:1 mixtures of chloroform and tri-fluoro-ethanol (TFE). Ibuprofen was also dissolved in a mixture of 1:1 chloroform and TFE. The DMPC, cholesterol and ibuprofen solutions were then mixed in the appropriate ratios to achieve the desired membrane compositions for the experiment. All samples prepared for this study are listed in Table 2. Molecular representations of the components are shown in Figure 1 (a).

A tilting incubator was heated to 313 K and the lipid solutions placed inside to equilibrate. 200 μ L of lipid solution was deposited on each wafer and the solvent was then allowed to slowly evaporate for ~10 minutes while being gently rocked, such that the lipid solution spread evenly on the wafers. After drying, the samples were

572 placed in vacuum at 313 K for 12 hours to remove all
 573 traces of solvent. Samples were then placed in a sealed
 574 container containing an open vial of pure water and al-
 575 lowed to equilibrate to 293 K. The temperature was then
 576 slowly increased to 303 K over a period of 24 hours. This
 577 procedure results in highly oriented, multi-lamellar mem-
 578 brane stacks on a uniform coverage of the silicon sub-
 579 strates. About 3000 highly oriented stacked membranes
 580 with a total thickness of $\sim 10 \mu\text{m}$ are produced using this
 581 protocol. The high sample quality and high degree of
 582 order is a prerequisite to determine in-plane and out-of-
 583 plane structure of the membranes separately, but simul-
 584 taneously.

585 4.2. X-Ray Scattering Experiment

586 Out-of-plane and in-plane X-ray scattering data was
 587 obtained using the Biological Large Angle Diffraction Ex-
 588 periment (BLADE) in the Laboratory for Membrane and
 589 Protein Dynamics at McMaster University. BLADE uses
 590 a 9kW (45 kV, 200 mA) CuK- α Rigaku Smartlab rotat-
 591 ing anode at a wavelength of 1.5418 Å. Both source and
 592 detector are mounted on moveable arms such that the
 593 membranes stay horizontal during measurements. Foc-
 594 cussing, multi layer optics provide a high intensity paral-
 595 lel beam with monochromatic X-ray intensities up to 10^{10}
 596 counts/(s \times mm 2). This beam geometry provides opti-
 597 mal illumination of the membrane samples to maximize
 598 the scattered signal. By using highly-oriented stacks, the
 599 in-plane (q_{\parallel}) and out-of-plane (q_z) structure of the mem-
 600 branes could be determined independently. A sketch of
 601 the scattering geometry is depicted in Figure 1 (b). Full
 602 2-dimensional reciprocal space maps are shown in Fig-
 603 ure 2.

604 The X-ray scattering experiments determine three
 605 pieces of information relevant to molecular structure of
 606 the membranes. Firstly, out-of-plane diffraction scans al-
 607 low for the identification of the phase of the membranes
 608 (lamellar or cubic) and also permit the reconstruction of
 609 electron density profiles (for lamellar samples). Electron
 610 density profiles were used to determine the position of
 611 the molecular constituents. Secondly, in-plane scatter-
 612 ing measurements at high q_{\parallel} allow for the organization
 613 of the lipid molecules in the plane of the membrane to
 614 be determined. The area per lipid may be determined
 615 from the in-plane structure, as detailed in Barrett *et al.*¹⁰.
 616 Thirdly, scans performed at low q_{\parallel} and low q_z can be used
 617 to measure the degree of orientation within the samples.

618 The 2-dimensional X-ray data in Figure 2 show well-
 619 defined peaks along the q_{\parallel} -axis, which allow the deter-
 620 mination of the lateral membrane structure. Several cor-
 621 relation peaks were observed in the in-plane data for
 622 ibuprofen concentrations of less than 2 mol%, and were
 623 well fit by Lorentzian peak profiles. The intensity has
 624 a distinct rod-like shape, typical for a 2-dimensional sys-
 625 tem. Membranes containing more than 2 mol% ibuprofen
 626 showed one broad Lorentzian peak, centered at $\sim 1.5 \text{ \AA}^{-1}$

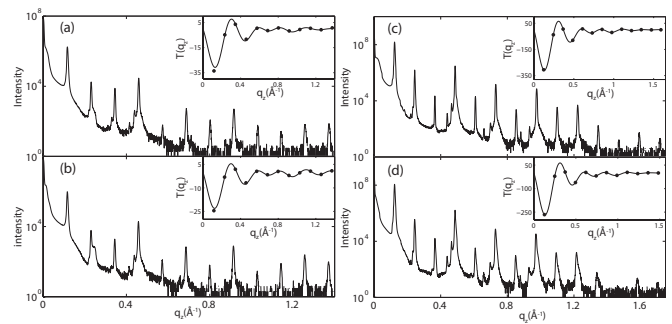


FIG. 10. Out-of-plane diffraction data for all samples for which Fourier analysis was performed. $T(q_z)$, which is proportional to the membrane form factor, is shown in each inset and was used to determine the phases ν_n . (a) pure DMPC; (b) 2 mol% ibuprofen; (c) 20 mol% cholesterol; (d) 20 mol% cholesterol and 20 mol% ibuprofen

627 due to the organization of the lipid tails in the hydropho-
 628 bic membrane core. The area per lipid molecule can be
 629 determined from the in-plane diffraction data, when as-
 630 suming that the lipid tails form a densely packed struc-
 631 ture with hexagonal symmetry (planar group p6), as re-
 632 ported from, e.g., neutron diffraction²⁶. In the absence
 633 of fluctuations (in gel state lipid bilayers), the area per
 634 lipid molecule can be determined from the position of the
 635 in-plane Bragg peak at q_T to $A_L = 16\pi^2/(\sqrt{3}q_T^2)$ ^{10,13,52}.
 636 The distance between two acyl tails is determined to be
 637 $a_T = 4\pi/(\sqrt{3}q_T)$, with the area per lipid simplified to
 638 $A_L = \sqrt{3}a_T^2$, as listed in Table 2. The area per lipid for
 639 the pure DMPC and DMPC+2 mol% ibuprofen samples,
 640 which show a highly organized lateral membrane struc-
 641 ture with additional in-plane Bragg peaks in Figure 2,
 642 were determined from the lattice parameters of the cor-
 643 responding orthogonal tail lattice.

644 Structural parameters measured using the diffraction
 645 measurements, such as d_z spacing and A_L , for all samples
 646 are provided in Table 2.

647 4.3. Out-of-Plane Structure and Electron Densities

648 The out-of-plane structure of the membranes was de-
 649 termined using out-of-plane X-ray diffraction. The mem-
 650 brane electron density, $\rho(z)$, is approximated by a 1-
 651 dimensional Fourier analysis:

$$\begin{aligned} \rho(z) &= \rho_W + \frac{F(0)}{d_z} + \frac{2}{d_z} \sum_{n=1}^N F(q_n) \nu_n \cos(q_n z) \\ &= \rho_W + \frac{F(0)}{d_z} + \frac{2}{d_z} \sum_{n=1}^N \sqrt{I_n q_n} \nu_n \cos\left(\frac{2\pi n z}{d_z}\right). \end{aligned} \quad (1)$$

652 N is the highest order of the Bragg peaks observed in
 653 the experiment and ρ_W is the electron density of bulk
 654 water. The integrated peak intensities, I_n , are multiplied
 655 by q_n to generate the form factors, $F(q_n)$. The bilayer

666 form factor which is in general a complex quantity, is
 667 real-valued when the structure is centro-symmetric. The
 668 phase problem of crystallography, therefore, simplifies to
 669 the sign problem $F(q_z) = \pm|F(q_z)|$ and the phases, ν_n ,
 660 can only take the values ± 1 . The phases, ν_n are needed
 661 to reconstruct the electron density profile from the scat-
 662 tering data following Eq. (1). When the membrane form
 663 factor $F(q_z)$ is measured at several q_z values in a contin-
 664 uous fashion, $T(q_z)$, which is proportional to $F(q_z)$, can
 665 be fit to the data:

$$T(q_z) = \sum_n \sqrt{I_n q_n} \operatorname{sinc}\left(\frac{1}{2}d_z q_z - \pi n\right). \quad (2)$$

666 In order to determine the phases quantitatively, the form
 667 factor has to be measured at different q_z -values using
 668 the so-called swelling technique or by measuring the bi-
 669 layer at different contrast conditions when using neutron
 670 diffraction. In this paper, by fitting the experimental
 671 peak intensities and comparing them to the analytical
 672 expression for $T(q_z)$ in Eq. (2), the phases, ν_n , could be
 673 assessed. Good agreement was obtained, and the results
 674 shown in Figure 10.

675 The calculated electron densities, $\rho(z)$, which are ini-
 676 tially on an arbitrary scale, were then transformed to an
 677 absolute scale. The curves were vertically shifted to fulfil
 678 the condition $\rho(0) = 0.22 \text{ e}^-/\text{\AA}^3$ (the electron density

679 of a CH_3 group) in the centre of a bilayer. The curves
 680 were then scaled until the total number of electrons e^-
 681 $= A_L \int_0^{d_z/2} \rho(z) dz$ across a membrane leaflet agrees with
 682 the total number of electrons expected based on the sam-
 683 ple composition, with the addition of 7 water molecules,
 684 in agreement with^{16,53}.

685 The d_z -spacing between two neighbouring membranes
 686 in the stack was determined from the distance between
 687 the Bragg reflections ($d_z = 2\pi/\Delta q_z$) along the out-of-
 688 plane axis, q_z . Up to a peak order of 12 was observed
 689 from DMPC membranes, and up to 14 for DMPC mem-
 690 branes with cholesterol. Note that not all diffraction or-
 691 ders are necessarily observed for the different samples as
 692 the scattering intensity depends on the form factor of the
 693 bilayers.

ACKNOWLEDGMENTS

695 This research was funded by the Natural Sciences and
 696 Engineering Research Council (NSERC) of Canada, the
 697 National Research Council (NRC), the Canada Founda-
 698 tion for Innovation (CFI), and the Ontario Ministry of
 699 Economic Development and Innovation. R.J.A. is the re-
 700 cipient of an Ontario Graduate Scholarship, L.T. is the
 701 recipient of a Canada Graduate Scholarship, M.C.R. is
 702 the recipient of an Early Researcher Award from the
 703 Province of Ontario.

-
- 704 ¹ Pereira-Leite C, Nunes C, Reis S (2013) Interaction of
 705 nonsteroidal anti-inflammatory drugs with membranes: *In*
 706 *vitro* assessment and relevance for their biological actions.
 707 *Progress in lipid research* 52: 571–584.
 708 ² Seydel J, Wiese M (2002) Drug-Membrane Interactions.
 709 Germany: Wiley-VCH.
 710 ³ Lichtenberger LM, Zhou Y, Jayaraman V, Doyen JR,
 711 O’Neil RG, et al. (2012) Insight into nsaid-induced mem-
 712 brane alterations, pathogenesis and therapeutics: char-
 713 acterization of interaction of nsais with phosphatidyl-
 714 choline. *BBA-MOL CELL BIOL L* 1821: 994–1002.
 715 ⁴ Goldstein D (1984) The effects of drugs on membrane flu-
 716 idity. *Ann Rev Pharmacol Toxicol* 24.
 717 ⁵ Frydman JNG, Fonseca AdSd, Rocha VCd, Benarroz MO,
 718 Rocha GdS, et al. (2010) Acetylsalicylic acid and morphol-
 719 ogy of red blood cells. *Brazilian Archives of Biology and*
 720 *Technology* 53: 575–582.
 721 ⁶ Zhou Y, Cho KJ, Plowman SJ, Hancock JF (2012) Non-
 722 steroidal anti-inflammatory drugs alter the spatiotemporal
 723 organization of ras proteins on the plasma membrane.
 724 *Journal of Biological Chemistry* 287: 16586–16595.
 725 ⁷ Zhou Y, Plowman SJ, Lichtenberger LM, Hancock JF
 726 (2010) The anti-inflammatory drug indomethacin alters
 727 nanoclustering in synthetic and cell plasma membranes.
 728 *Journal of Biological Chemistry* 285: 35188–35195.
 729 ⁸ Rheinstädter MC, Schmalzl K, Wood K, Strauch D (2009)
 730 Protein-protein interaction in purple membrane. *Phys Rev*
 731 *Lett* 103: 128104.
 732 ⁹ Armstrong CL, Sandqvist E, Rheinstädter MC (2011)
 733 Protein-protein interactions in membranes. *Protein Pept*
 734 *Lett* 18: 344–353.
 735 ¹⁰ Barrett M, Zheng S, Roshankar G, Alsop R, Belanger R,
 736 et al. (2012) Interaction of aspirin (acetylsalicylic acid)
 737 with lipid membranes. *PLoS ONE* 7: e34357.
 738 ¹¹ Suwalsky M, Belmar J, Villena F, Gallardo MJ, Jemiola-
 739 Rzeminska M, et al. (2013) Acetylsalicylic acid (aspirin)
 740 and salicylic acid interaction with the human erythrocyte
 741 membrane bilayer induce *in vitro* changes in the morphol-
 742 ogy of erythrocytes. *Archives of biochemistry and biophysics*
 743 539: 9–19.
 744 ¹² Alsop RJ, Barrett MA, Zheng S, Dies H, Rheinstädter MC
 745 (2014) Acetylsalicylic acid (asa) increases the solubility of
 746 cholesterol when incorporated in lipid membranes. *Soft*
 747 *matter* 10: 4275–4286.
 748 ¹³ Barrett M, Zheng S, Topozini L, Alsop R, Dies H, et al.
 749 (2013) Solubility of cholesterol in lipid membranes and the
 750 formation of immiscible cholesterol plaques at high choles-
 751 terol concentrations. *Soft Matter* 9: 9342 - 9351.
 752 ¹⁴ Alsop RJ, Topozini L, Marquardt D, Kučerka N, Harroun
 753 TA, et al. (2014) Aspirin inhibits formation of cholesterol
 754 rafts in fluid lipid membranes. *Biochimica et Biophysica*
 755 *Acta (BBA)-Biomembranes* .
 756 ¹⁵ Koltover I, Salditt T, Rädler JO, Safinya CR (1998) An in-
 757 verted hexagonal phase of cationic liposome-dna complexes
 758 related to dna release and delivery. *Science* 281: 78–81.
 759 ¹⁶ Dies H, Topozini L, Rheinstädter MC (2014) The inter-
 760 action between amyloid- β peptides and anionic lipid mem-

- branes containing cholesterol and melatonin. *PLoS one* 9: e99124.
- ¹⁷ Davies NM (1998) Clinical pharmacokinetics of ibuprofen. *Clinical pharmacokinetics* 34: 101–154.
- ¹⁸ Rome LH, Lands W (1975) Structural requirements for time-dependent inhibition of prostaglandin biosynthesis by anti-inflammatory drugs. *Proceedings of the National Academy of Sciences* 72: 4863–4865.
- ¹⁹ Boggara MB, Krishnamoorti R (2009) Small-angle neutron scattering studies of phospholipid- NSAID adducts. *Langmuir* 26: 5734–5745.
- ²⁰ Du L, Liu X, Huang W, Wang E (2006) A study on the interaction between ibuprofen and bilayer lipid membrane. *Electrochimica acta* 51: 5754–5760.
- ²¹ Boggara MB, Faraone A, Krishnamoorti R (2010) Effect of pH and ibuprofen on the phospholipid bilayer bending modulus. *The Journal of Physical Chemistry B* 114: 8061–8066.
- ²² Hristova K, White SH (1998) Determination of the hydrocarbon core structure of fluid dioleoylphosphocholine (dopc) bilayers by x-ray diffraction using specific bromination of the double-bonds: Effect of hydration. *Biophysical Journal* 74: 2419–2433.
- ²³ Katsaras J, Raghunathan VA, Dufourc EJ, Dufourcq J (1995) Evidence for a two-dimensional molecular lattice in subgel phase dppc bilayers. *Biochemistry (Mosc)* 34: 4684–4688.
- ²⁴ Raghunathan VA, Katsaras J (1995) Structure of the l'_c phase in a hydrated lipid multilamellar system. *Phys Rev Lett* 74: 4456–4459.
- ²⁵ Tristram-Nagle S, Liu Y, Legleiter J, Nagle JF (2002) Structure of gel phase dmpc determined by x-ray diffraction. *Biophys J* 83: 3324–3335.
- ²⁶ Armstrong CL, Marquardt D, Dies H, Kučerka N, Yamani Z, et al. (2013) The observation of highly ordered domains in membranes with cholesterol. *PLoS ONE* 8: e66162.
- ²⁷ Barbato F, La Rotonda MI, Quaglia F (1997) Interactions of nonsteroidal antiinflammatory drugs with phospholipids: comparison between octanol/buffer partition coefficients and chromatographic indexes on immobilized artificial membranes. *Journal of pharmaceutical sciences* 86: 225–229.
- ²⁸ Gaede HC, Gawrisch K (2003) Lateral diffusion rates of lipid, water, and a hydrophobic drug in a multilamellar liposome. *Biophysical journal* 85: 1734–1740.
- ²⁹ Shankland N, Wilson C, Florence A, Cox P (1997) Refinement of ibuprofen at 100k by single-crystal pulsed neutron diffraction. *Acta Crystallographica Section C: Crystal Structure Communications* 53: 951–954.
- ³⁰ Dies H, Cheung B, Tang J, Rheinstädter MC (2015) The organization of melatonin in lipid membranes. *Biochimica et Biophysica Acta (BBA)-Biomembranes* .
- ³¹ Armstrong CL, Häußler W, Seydel T, Katsaras J, Rheinstädter MC (2014) Nanosecond lipid dynamics in membranes containing cholesterol. *Soft matter* 10: 2600–2611.
- ³² Khajeh A, Modarress H (2014) The influence of cholesterol on interactions and dynamics of ibuprofen in a lipid bilayer. *Biochimica et Biophysica Acta (BBA)-Biomembranes* .
- ³³ Geraldo VP, Pavinatto FJ, Nobre TM, Caseli L, Oliveira ON (2013) Langmuir films containing ibuprofen and phospholipids. *Chemical Physics Letters* 559: 99–106.
- ³⁴ Kopeć W, Telenius J, Khandelia H (2013) Molecular dynamics simulations of the interactions of medicinal plant extracts and drugs with lipid bilayer membranes. *FEBS Journal* 280: 2785–2805.
- ³⁵ Hansen AH, Sørensen KT, Mathieu R, Serer A, Duelund L, et al. (2013) Propofol modulates the lipid phase transition and localizes near the headgroup of membranes. *Chemistry and physics of lipids* 175: 84–91.
- ³⁶ Lindblom G, Rilfors L (1989) Cubic phases and isotropic structures formed by membrane lipids possible biological relevance. *Biochimica et Biophysica Acta (BBA)-Reviews on Biomembranes* 988: 221–256.
- ³⁷ Shearman G, Tyler A, Brooks N, Templer R, Ces O, et al. (2010) Ordered micellar and inverse micellar lyotropic phases. *Liquid Crystals* 37: 679–694.
- ³⁸ Morris M (2014) Directed self-assembly of block copolymers for nanocircuitry fabrication. *Microelectronic Engineering* .
- ³⁹ Squires AM, Templer R, Seddon J, Woenckhaus J, Winter R, et al. (2002) Kinetics and mechanism of the lamellar to gyroid inverse bicontinuous cubic phase transition. *Langmuir* 18: 7384–7392.
- ⁴⁰ Conn CE, Ces O, Mulet X, Finet S, Winter R, et al. (2006) Dynamics of structural transformations between lamellar and inverse bicontinuous cubic lyotropic phases. *Physical review letters* 96: 108102.
- ⁴¹ Montalvo G, Pons R, Zhang G, Díaz M, Valiente M (2013) Structure and phase equilibria of the soybean lecithin/peg 40 monostearate/water system. *Langmuir* 29: 14369–14379.
- ⁴² Gillams RJ, Nylander T, Plivelic TS, Dymond MK, Attard GS (2014) Formation of inverse topology lyotropic phases in dioleoylphosphatidylcholine/oleic acid and dioleoylphosphatidylethanolamine/oleic acid binary mixtures. *Langmuir* 30: 3337–3344.
- ⁴³ Schmidt NW, Wong GC (2013) Antimicrobial peptides and induced membrane curvature: Geometry, coordination chemistry, and molecular engineering. *Current Opinion in Solid State and Materials Science* 17: 151–163.
- ⁴⁴ Kulkarni CV (2011) Nanostructural studies on monoolein–water systems at low temperatures. *Langmuir* 27: 11790–11800.
- ⁴⁵ Raçon Y, Charvolin J (1988) Epitaxial relationships during phase transformations in a lyotropic liquid crystal. *The Journal of Physical Chemistry* 92: 2646–2651.
- ⁴⁶ Squires AM, Hallett JE, Beddoes CM, Plivelic TS, Seddon AM (2013) Preparation of films of a highly aligned lipid cubic phase. *Langmuir* 29: 1726–1731.
- ⁴⁷ Angelov B, Angelova A, Vainio U, Garamus VM, Lesieur S, et al. (2009) Long-living intermediates during a lamellar to a diamond-cubic lipid phase transition: a small-angle x-ray scattering investigation. *Langmuir* 25: 3734–3742.
- ⁴⁸ Yoneyama F, Shioya K, Zendo T, Nakayama J, Sonomoto K (2010) Effect of a negatively charged lipid on membrane-lactacin q interaction and resulting pore formation. *Bio-science, biotechnology, and biochemistry* 74: 218–221.
- ⁴⁹ Bernsdorff C, Reszka R, Winter R (1999) Interaction of the anticancer agent taxol (paclitaxel) with phospholipid bilayers. *Journal of biomedical materials research* 46: 141–149.
- ⁵⁰ Bloch KE (1983) Sterol, structure and membrane function. *Crit Rev Biochem Mol Biol* 14: 47–92.
- ⁵¹ Tenchov BG, MacDonald RC, Siegel DP (2006) Cubic phases in phosphatidylcholine-cholesterol mixtures: cholesterol as membrane fusogen. *Biophysical journal* 91: 2508–2516.

- ⁸⁸⁸ ⁵² Mills TT, Toombes GES, Tristram-Nagle S, Smilgies DM, ⁸⁹¹ x-ray scattering. *Biophys J* 95: 669-681.
- ⁸⁸⁹ Feigenson GW, et al. (2008) Order parameters and areas ⁸⁹² ⁵³ Nováková E, Giewekemeyer K, Salditt T (2006) Structure
- ⁸⁹⁰ in fluid-phase oriented lipid membranes using wide angle ⁸⁹³ of two-component lipid membranes on solid support: An
- ⁸⁹⁴ x-ray reflectivity study. *Phys Rev E* 74: 051911.

Graphical Abstract**Cholesterol Expels Ibuprofen from the Hydrophobic Membrane Core and Stabilizes Lamellar Phases in Lipid Membranes Containing Ibuprofen**

Richard J Alsop, Clare L Armstrong, Amna Maqbool, Laura Topozini, Hannah Dies and Maikel C Rheinstädter

Our experiments provide evidence for a non-specific interaction between ibuprofen and cholesterol in lipid membranes. Ibuprofen was found to reside in both the head group and tail group regions of the saturated DMPC bilayers. However, when cholesterol was incorporated in the membranes, ibuprofen was found to reside in the head group region, only. At the same time, cholesterol was found to stabilize the lamellar membrane phase by suppressing the transition into a cubic phase.

